

The southern edge of cratonic North America: Evidence from new satellite magnetometer observations

Michael Purucker,¹ Benoit Langlais,² Nils Olsen,³ Gauthier Hulot,⁴ and Mioara Mandea⁴

Received 16 June 2001; revised 5 October 2001; accepted 9 November 2001; published 14 May 2002.

[1] A global model is developed for both induced and remanent magnetizations in the terrestrial lithosphere. The model is compared with, and well-described by, Ørsted satellite observations. Interpretation of the observations over North America suggests that the large total field anomalies, associated with spherical harmonic degrees 15–26 and centered over Kentucky and the south-central United States, are the manifestations of the magnetic edges of the southern boundaries of cratonic North America. The techniques and models developed here may be of use in defining other cratonic boundaries. *INDEX TERMS*: 1545 Geomagnetism and Paleomagnetism: Spatial variations (all harmonics and anomalies); 1219 Geodesy and Gravity: Local gravity anomalies and crustal structure; 7218 Seismology: Lithosphere and upper mantle; 9350 Information Related to Geographic Region: North America

1. Background

[2] The launch of the Ørsted high-precision geomagnetic field satellite [Neubert *et al.*, 2001] has invigorated efforts to understand the magnetic field of the earth's lithosphere. Early attempts [Langel and Hinze, 1998] to model the lithospheric field relied on forward and inverse approaches over local regions. After the realization that much of the lithospheric magnetic signal might be obscured by overlap with the long-wavelength magnetic field from the core [Meyer *et al.*, 1985], recent work has explored the potential of global forward [Cohen and Achache, 1994; Dyment and Arkani-Hamed, 1998] and inverse models [Purucker *et al.*, 1998]. Our work elaborates on but differs from previous work which 1) included remanent magnetizations associated only with the Cretaceous Quiet Zones [Cohen and Achache, 1994; Purucker *et al.*, 1998], 2) did not consider induced magnetizations at all [Dyment and Arkani-Hamed, 1998], 3) used a model of induced magnetization that had fewer geologic and geophysical inputs [Purucker *et al.*, 1998].

2. A New Global Magnetization Model

[3] The global model of induced magnetization is based on an estimate of the volume of the magnetic crust and its magnetic susceptibility. We assume that induced magnetizations are restricted to the crust [Wasilewski and Mayhew, 1992] and utilize a global seismic tomography model [Nataf and Ricard, 1996] for estimating crustal thickness. The model also contains a tectonic-based subdivision of the crust into three categories, each of which has an associated geotherm. These geotherms, when coupled with

an assumption about the magnetic mineral(s) responsible for the bulk of the magnetization, allow for the calculation of a depth to the Curie isotherm. We assume here that the magnetic mineral is magnetite or low-Ti magnetite. The magnetic layer thickness is calculated as the thickness of the igneous crust above the magnetite Curie isotherm. We utilize a sediment thickness model [Laske and Masters, 1997] to account for the presence of effectively non-magnetic sediment or sedimentary rock which serves to decrease the effective magnetic layer thickness. Although we calculate our induced magnetization model globally, the models shown here depict only a hemisphere centered on North America because our interpretation will focus on this region (Figure 1a). We use magnetic susceptibility values of 0.035 SI for the continental crust and 0.04 SI for the oceanic lithosphere [Purucker *et al.*, 1998]. The resulting maps are not strongly sensitive to the exact choice of magnetic susceptibility contrast between oceans and continents.

[4] The remanent magnetization model is restricted to the oceanic lithosphere, not because of the lack of continental remanent magnetization [Clark, 1999], but because not enough is known of continental remanent magnetization to make a global model. The oceanic remanent model [Dyment and Arkani-Hamed, 1998] that we use is based on non-satellite magnetic input and has been subsequently calibrated using observed Magsat anomalies in the South Atlantic ocean [Purucker and Dyment, 2000]. The remanent model consists of magnetization vector direction and intensity. The vector direction and its variation with paleolatitude have been determined using ocean floor ages, relative motion parameters for each plate, and the apparent paleomagnetic polar wander path for Africa. The total field calculated from the remanent magnetization model is shown at 400 km in Figure 1b.

[5] The sum of the total field from the induced and remanent models is shown in Figure 1c. Because the core field overlaps with the lithospheric field between degrees 1–14 we discard those degrees [Arkani-Hamed *et al.*, 1994], as well as all degrees greater than 26 (to be consistent with the satellite observations discussed below). The remaining total fields of lithospheric origin are shown in Figure 1d.

3. New Satellite Magnetic Field Observations

[6] Maps of the magnetic field from Magsat (Years: 1979–1980) and Ørsted (Years: 1999–present) spacecraft missions are based on sets of spherical harmonic coefficients, estimated using geomagnetically quiet, night-time, vector and scalar observations. The Magsat map, termed M102389, [Cain *et al.*, 1990] estimated static fields to degree and order 49 while the Ørsted map estimates static fields to degree and order 29. The Ørsted map uses techniques described in Olsen *et al.* [2000]. Additional techniques and data utilized for this Ørsted map include iteratively reweighted least-squares with Huber weights and the incorporation of satellite data from March, 1999–March, 2001. We also incorporate ground magnetic observatory data. The secular variation model is of degree 13. We consider the Ørsted map robust through at least degree 26 and so for comparison we truncate both maps at degree 26. Earlier Ørsted maps [Olsen *et al.*, 2000; Langlais, personal communication] show many of the same features as the new maps.

¹Raytheon ITSS at Geodynamics Branch, Goddard Space Flight Center, Greenbelt, MD, USA.

²NAS/NRC at Geodynamics Branch, Goddard Space Flight Center, Greenbelt, MD, USA.

³Danish Space Research Institute, Copenhagen, Denmark.

⁴Institut de Physique du Globe de Paris, Paris cedex 05, France.

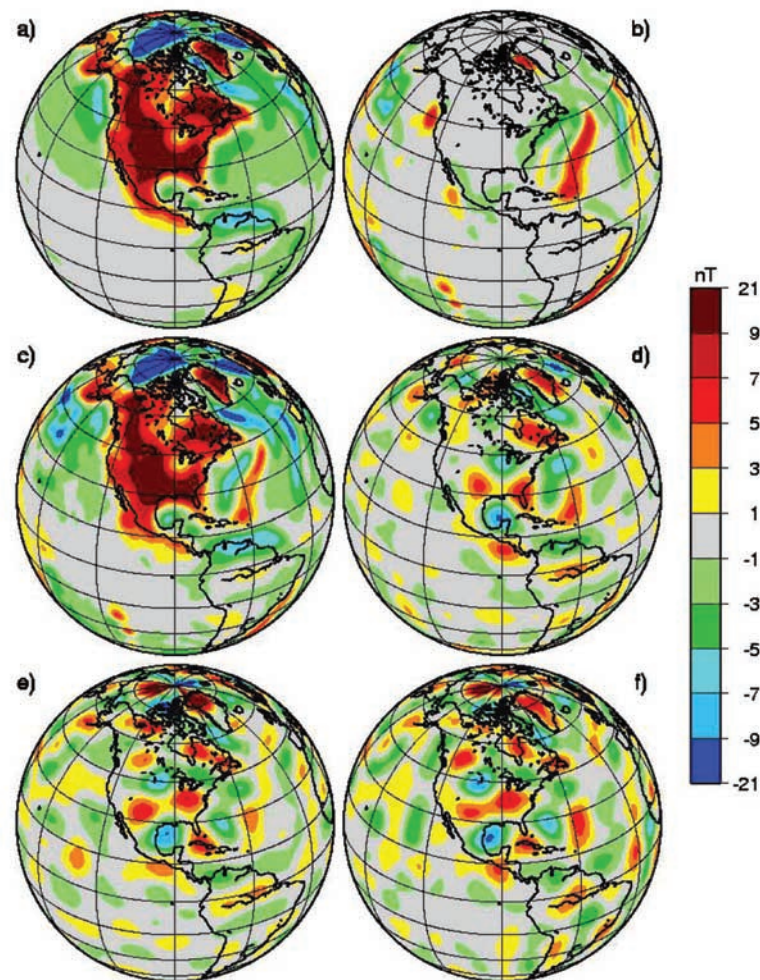


Figure 1. (a) A map of the modeled magnetic field (all harmonics) due to induced magnetization. (b) A map of the modeled magnetic field (all harmonics) due to remanent magnetization in the oceans. (c) The sum of induced and remanent magnetizations (all harmonics). (d) Induced and remanent magnetization model between degrees 15 and 26. (e) The magnetic field as measured by Magsat between degrees 15 and 26. (f) The magnetic field as measured by Ørsted between degrees 15 and 26. Features poleward of 83 degrees latitude are less reliable because the inclination of the satellites was approximately 97 degrees. All maps are of the total field and are shown at an altitude of 400 km using an orthographic projection centered at 90 degrees West, 30 degrees North.

We again discard the field originating largely in the core (Degrees 1–14) and the resulting maps from Magsat (Figure 1e) and Ørsted (Figure 1f) are shown for comparison with the models. The global correlation (in the spherical harmonic domain) between these two maps generally ranges from 0.65 to 0.85, with only two degrees (18 and 26) showing lower but still significant correlations (0.5 to 0.6).

4. Derivation of Improved Magnetization Maps

[7] The major features shown in the observations of Figures 1e and 1f show an almost one-to-one correspondence to the model's features shown in Figure 1d. The model is closest to the observations over North America and the North Atlantic Ocean, in contrast to the North Pacific [Yanez and LaBrecque, 1997] where the observations record stronger magnetic signatures than predicted by the model. In North America (Figure 2), the model high centered over Georgia (Figure 2b) appears to be the same feature as that centered over the Kentucky region in the observations (Figures 1e and 1f), but shifted slightly to the northwest. This difference may be a consequence of the crude three-fold thermal subdivision provided by the global seismic tomography model [Nataf and Ricard, 1996]. This subdivision divides the continental

crust into 1) Archean-floored (>1.7 Ga) with a heat flow that produces a magnetite Curie isotherm at 81 km, 2) Younger but still stable crust (0.25 to 1.7 Ga) with a heat flow that corresponds to a magnetite Curie isotherm at 58 km depth, and 3) basement younger than 0.25 Ga with a heat flow that yields a magnetite Curie isotherm at 29 km depth. As in any potential field inverse problem, there are several possible ways in which the crustal model, the magnetic thickness of which is shown in Figure 2a, might be modified to more closely fit the observations. One possibility is an increase in magnetic thickness over the Kentucky region and a decrease over Georgia [Purucker et al., 1998]. This is equivalent to enhanced magnetic susceptibilities or magnetizations over Kentucky and proportionally weaker ones over Georgia. Another option is to markedly reduce the magnetic thickness over Georgia, Florida, and the rest of the Atlantic and Gulf Coastal Plains. This is appealing because this corresponds to decreasing the magnetic thickness over non-magnetic sedimentary rocks of the coastal plain, while retaining the original model thickness over the magnetic igneous and metamorphic rocks of the adjacent Piedmont (Figure 2a). This would be consistent with the fact that the surface boundary between these two regions is 50–150 km east of a prominent regional Bouguer gravity gradient, inferred to represent

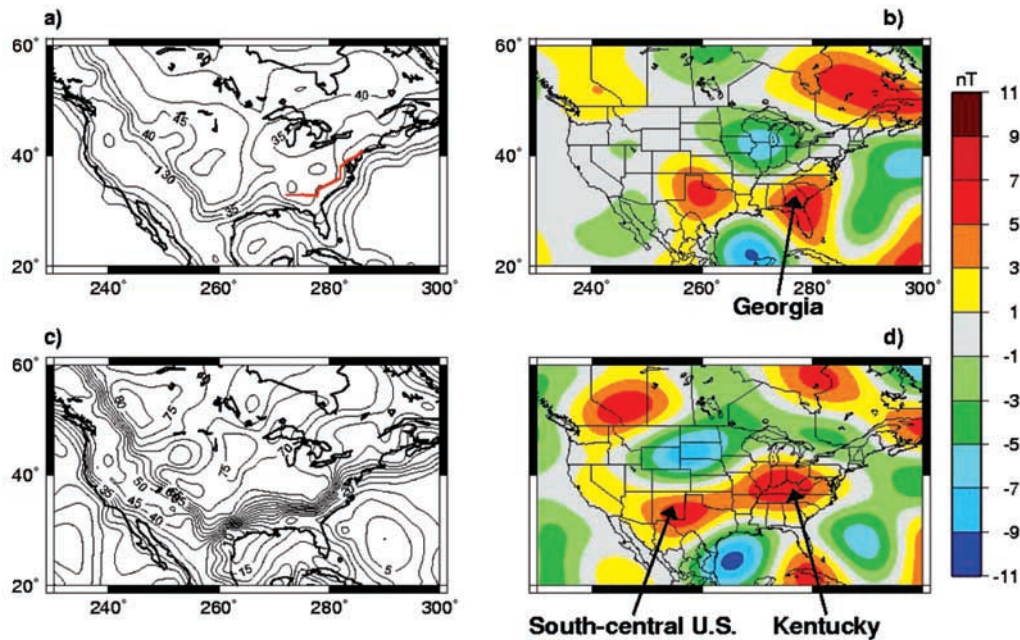


Figure 2. (a) A map of the magnetic crustal thickness from the initial induced magnetization model (5 km contour interval) over the North American region. The solid red line locates the boundary between the relatively non-magnetic sediments of the Coastal Plain and the inboard, more magnetic igneous and metamorphic rocks. (b) the magnetic field calculated from initial induced (Figure 2a) and remanent magnetization model. (c) The vertically integrated magnetization model (shown in color as Figure 3) that explains the satellite observations over the North American region (5 kA contour interval), and (d) the magnetic field calculated from the vertically integrated magnetization model of Figure 2c. The RMS misfit between this map and the observations (Figure 1f) is 0.5 nT while the maximum difference between the two maps is 1.5 nT. All maps are shown using a Cylindrical Equidistant projection centered at 95 West Longitude. All magnetic field maps are of the total field at 400 km altitude and are shown between degrees 15 and 26.

the buried edge of the deep Precambrian craton in the Appalachian orogen [Hinze and Zietz, 1985].

[8] An iterative inverse approach was developed [Purucker *et al.*, 1998] that will generate a vertically integrated magnetization model which reproduces the measured field to any desired precision. However, this approach will modify wavelength components that are largely within the measurement range (spherical harmonic degrees 15–26). We utilize other geological and geophysical data sets to modify the longer wavelengths, and make a final correction to the model using the Ørsted magnetics data alone in an iterative inverse approach. Adopting this approach, we modify (i.e. edit by hand) our initial model so as to place the boundary between thicker (35 km) and thinner (12 km) magnetic crust at the inboard Coastal plain boundary. The final correction to our model is based on differencing the magnetic observations and the total field of the modified model. This difference is globally modeled for magnetizations using an iterative equivalent source approach [Purucker *et al.*, 1996]. The resulting vertically integrated magnetization solution (Figures 2c and 3) is an example of a global magnetization model that simultaneously fits the spacecraft observations (Figure 1f), other geological and geophysical knowledge on the near surface and depth extent of the magnetic sources, and has the virtue of simplicity.

5. Interpretation

[9] Previous interpretations of the southeastern U.S. region [Mayhew *et al.*, 1985; Ruder and Alexander, 1986], using forward and inverse modeling approaches, invoked enhanced magnetizations (1–4 A/m over a thickness of 10–30 km) in the Kentucky and Tennessee regions, paired with weaker magnetizations over the Georgia region. We suggest here an interpretation of the satellite observations that explains the Kentucky total intensity high as a

manifestation of the magnetic edge of the southeast corner of cratonic North America. The magnetic boundary, shown as the steep gradient in Figures 2c and 3, is located close to the maximum gravity gradient and the geologic boundary between magnetic and non-magnetic surficial rocks. At an altitude of 400 km, the magnitude of the Kentucky anomaly is 7 nT in the model, and in the Ørsted and Magsat observations. Additional power can be seen at higher harmonic degree (for example, in Magsat and in aeromagnetic surveys of North America) and this probably indicates the presence of enhanced magnetization locally in Kentucky. But the feature seen by the new Ørsted satellite observations, from spherical harmonic degrees 15–26, can be explained without invoking enhanced magnetizations. This suggests that the Kentucky anomaly as seen by Magsat (degrees 15–40 total field anomaly increased by 3 nT and center shifts by about 2 degrees relative to the position and strength shown here) has two distinct origins. While such an interpretation might also have been made from the earlier Magsat satellite observations, the lower resolution view afforded by Ørsted allows for regional interpretations uncomplicated by local features. In a similar way, the high over the south-central United States (Figures 2b and 2d) is a manifestation of the southwest corner of cratonic North America. Another prominent feature on the new magnetization model (Figures 2c and 3) is the enhanced vertically integrated magnetization over the Mid-continent high [Hinze and Zietz, 1985], a prominent gravity and magnetic high on near-surface maps that is not normally seen on satellite magnetic maps. The new model is available at http://core2.gsfc.nasa.gov/research/purucker/craton_edge.html.

[10] The magnetization distribution in Figure 3 is very different from estimates made using simple local inversion schemes unconstrained by information on the local geology and geophysics. It illustrates the difficulty of inferring magnetization distributions from magnetic field observations, especially in cases where mag-

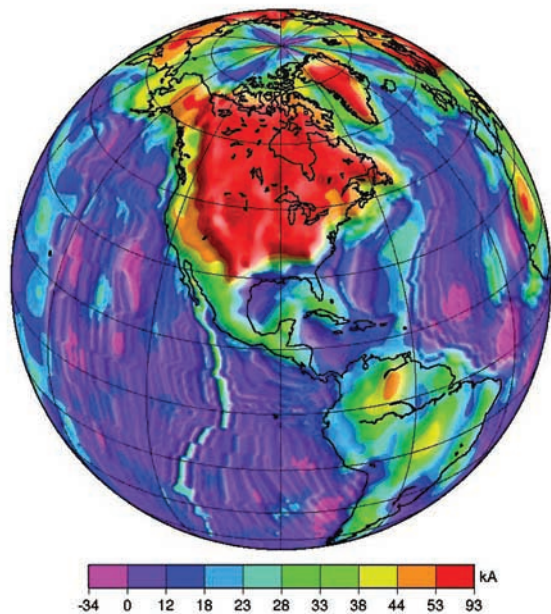


Figure 3. A vertically-integrated magnetization model of induced and remanent magnetization that explains the satellite magnetic field observations. The model also incorporates information from near-surface magnetic field observations. Areas of negative magnetization are dominated by magnetizations in directions oblique and opposite to that of the present earth's field. The model shows the long-wavelength magnetizations (dominated by the continent-ocean contrast) in color and the short wavelength magnetizations (dominated by seafloor spreading) as a gray-scale shaded relief. The map is shown on an orthographic projection centered at 90 degrees West, 30 degrees North. A contour map of this same figure over North America is shown as Figure 2c.

netic fields of multiple origins are superimposed. Finally, the explanation of the large total field anomalies over southern North America as being due to induced magnetization alone make the large remanent magnetic anomalies at Mars [Purucker *et al.*, 2000] even more enigmatic.

[11] **Acknowledgments.** We thank J. LaBrecque, D. Ravat, and two anonymous reviewers for comments on this manuscript. Supported by NASA contract NAS5-99010 to M. Purucker. This is IGP contribution number 1798.

References

Arkani-Hamed, J., R. A. Langel, and M. Purucker, Scalar magnetic anomaly maps of Earth derived from POGO and Magsat data, *J. Geophys. Res.*, *99*, 24,075–24,090, 1994.
Cain, J. C., B. Holter, and D. Sandee, Numerical experiments in geomagnetic modeling, *J. Geomag. Geoelectr.*, *42*, 973–987, 1990.

Clark, D. A., Magnetic petrology of igneous intrusions: Implications for exploration and magnetic interpretation, *Exploration Geophysics*, *30*, 5–26, 1999.
Cohen, Y., and J. Achache, Contribution of induced and remanent magnetization to long-wavelength oceanic magnetic anomalies, *J. Geophys. Res.*, *99*, 2943–2954, 1994.
Dyment, J., and J. Arkani-Hamed, Contribution of lithospheric remanent magnetization to satellite magnetic anomalies over the world's oceans, *J. Geophys. Res.*, *103*, 15,423–15,441, 1998.
Hinze, W. J., and I. Zietz, The composite magnetic anomaly map of the conterminous United States, in *The Utility of Regional Gravity and Magnetic Anomaly Maps*, edited by W. J. Hinze, pp. 1–24, Soc. Of Expl. Geophys., Tulsa, OK, 1985.
Langel, R. A., and W. J. Hinze, The magnetic field of the earth's lithosphere: The satellite perspective, 429 pp., Cambridge University Press, 1998.
Laske, G., and G. Masters, A global digital map of sediment thickness (abstract), *EOS Trans. AGU*, *78*, Fall Meet. Suppl., F483, 1997.
Mayhew, M. A., R. H. Estes, and D. M. Myers, Magnetization models for the source of the "Kentucky anomaly" observed by Magsat, *Earth Planet. Sci. Lett.*, *74*, 117–129, 1985.
Meyer, J., J. H. Hufen, M. Siebert, and A. Hahn, On the identification of Magsat anomaly charts as crustal part of internal field, *J. Geophys. Res.*, *90*, 2537–2542, 1985.
Nataf, H., and Y. Ricard, 3SMAC: An a priori tomographic model of the upper mantle based on geophysical modeling, *Phys. Earth Planet. Int.*, *95*, 101–122, 1996.
Neubert, T., M. Manda, G. Hulot, R. von Frese, F. Prindahl, J. L. Jorgensen, E. Friis-Christensen, P. Stauning, N. Olsen, and T. Risbo, Ørsted satellite captures high-precision geomagnetic field data, *Eos Trans. AGU*, *82*(7), 81–88, 2001.
Olsen, N., et al., Ørsted initial field model, *Geophys. Res. Lett.*, *27*, 3607–3610, 2000.
Purucker, M. E., T. J. Sabaka, and R. A. Langel, Conjugate gradient analysis: A new tool for studying satellite magnetic data sets, *Geophys. Res. Lett.*, *23*, 507–510, 1996.
Purucker, M. E., R. A. Langel, M. Rajaram, and C. Raymond, Global magnetization models with a priori information, *J. Geophys. Res.*, *103*, 2563–2584, 1998.
Purucker, M., D. Ravat, H. Frey, C. Voorhies, T. Sabaka, and M. Acuna, An altitude-normalized magnetic map of Mars and its interpretation, *Geophys. Res. Lett.*, *27*, 2449–2452, 2000.
Purucker, M. E., and J. Dyment, Satellite magnetic anomalies related to seafloor spreading in the South Atlantic Ocean, *Geophys. Res. Lett.*, *27*, 2765–2768, 2000.
Ruder, M. E., and S. S. Alexander, Magsat equivalent source anomalies over the southeastern United States: Implications for crustal magnetization, *Earth and Plan. Sci. Lett.*, *78*, 33–43, 1986.
Wasilewski, P. J., and M. A. Mayhew, The Moho as a magnetic boundary revisited, *Geophys. Res. Lett.*, *19*, 2259–2262, 1992.
Yanez, G. A., and J. L. LaBrecque, Age-dependent three-dimensional magnetic modeling of the North Pacific and North Atlantic oceanic crust at intermediate wavelengths, *J. Geophys. Res.*, *102*, 7947–7961, 1997.

M. Purucker, Raytheon ITSS at Geodynamics Branch, Goddard Space Flight Center, Greenbelt, MD 20771, USA.

B. Langlais, Geodynamics Branch, Goddard Space Flight Center, Greenbelt, MD 20771, USA.

G. Hulot and M. Manda, Institut de Physique du Globe de Paris, 4 Place Jussieu, 75252, Paris cedex 05, France.

N. Olsen, Danish Space Research Institute, Juliane Maries Vej 30, DK-2100 Copenhagen, Denmark.